# Incorporation of Partially Hydrolyzed Polyacrylamide With Zwitterionic Units and Poly(Ethylene Glycol) Units Toward Enhanced Tolerances to High Salinity and High Temperature

Gang Lu[1,2], Jikuan Zhao[3]*, Shaoqi Li[3], Yuquan Chen[3], Chunfang Li[3], Youqi Wang[1,2] and Dongxiang Li[4]*

[1]State Key Laboratory of Shale Oil and Gas Enrichment Mechanisms and Effective Development, Beijing, China, [2]Research and Development Center for the Sustainable Development of Continental Sandstone Mature Oilfield by National Energy Administration, Beijing, China, [3]College of Chemistry and Molecular Engineering, Qingdao University of Science and Technology, Qingdao, China, [4]State Key Laboratory Base of Eco-chemical Engineering, Qingdao University of Science and Technology, Qingdao, China

Partially hydrolyzed polyacrylamide (HPAM) was widely implemented to improve the rheological properties of displacing fluids, but the high temperature and salinity of the reservoir brine limited their applications. Herein, copolymers including HPAM, zwitterion-modified HPAM (z-HPAM), PEG-modified HPAM (p-HPAM), and zwitterion/PEG-modified HPAM (zp-HPAM) were prepared by free radical polymerization in an aqueous solution. The viscosity of these copolymers under different temperature and salinity was measured in aqueous solution. It is found that the viscosity of the HPAM under the harsh condition (90°C, $20 \times 10^4$ mg/L salinity) is only 9.6% of that value under the normal condition (25°C, pure water), while the z-HPAM can significantly improve salt resistance by the effects of salting-in effect and intermolecular electrostatic crosslinking, showing a viscosity retention of 22.9% under the harsh condition. The addition of PEG-containing monomer can strengthen hydrogen bonding between the polymer chains and form a sterically ordered structure with improved salinity and temperature resistance. The synergistic effect of zwitterion units and PEG units endows the zp-HPAM with good salinity and temperature resistance; thus, the sample viscosity under the harsh condition remains 170 mPa s, which retains 29% of the value under the normal condition. The enhanced rheology properties of the zp-HPAM under the harsh condition are significant for the enhanced oil recovery of water-soluble polymer flooding.

Keywords: partially hydrolyzed polyacrylamide, viscosity, high salinity and high temperature, zwitteronic polymer, poly(ethylene glycol)

## INTRODUCTION

Polymer flooding has better viscoelasticity and better sweep efficiency than simple water flooding for the enhanced oil recovery (Wever et al., 2011; Abidin et al., 2012; Wang et al., 2019). Especially in recent decades, water-soluble polymers such as partially hydrolyzed polyacrylamide (HPAM) have been widely implemented to improve the rheological properties of displacing fluids. However, such

HPAM flooding system is limited by temperature and salinity of the reservoir brine because the viscosity of the displacing fluids will be severely reduced under the harsh conditions above 75°C and $3 \times 10^4$ mg/L salinity in most oil reservoirs (Kamal et al., 2015). There are many reasons for the viscosity loss of water-soluble polymer fluids. For example, at high temperatures, (1) some polymer molecules will undergo thermal degradation and hydrolysis, and then the shortening of the polymer chain will result in a significant decrease in the intermolecular friction; (2) intensive thermal motion of the polymer chain reduces the stacking and tangling of the polymers; and (3) intensive thermal motion of solvent water molecules thins the hydration layer on the polymer chain, and the subsequent coiling and collapsing of the polymer chains cause the microscopic phase separation of the polymers from water. Otherwise, under a high salinity, (4) the strong "salting-out" effect promotes the phase separation of the polymers from water, because monovalent cations can shield the electrostatic repulsion among the carboxylate charges along the HPAM chains and compress the electric double layer of hydration film on the polymer surface, causing the polymer chain to coil and collapse (Liang et al., 2019); meanwhile, divalent ions, particularly $Ca^{2+}$ and $Mg^{2+}$, can complex with the carboxylate groups, leading to the precipitation of the HPAM chains in the brines (Peng and Wu, 1999).

In the past years, to overcome the negative impact of high temperature on the HPAM fluid systems, the concept of "thermoviscosifying polymer" was proposed to have a response to high temperature and bring a rise of the system viscosity (L'Alloret et al., 1995; Hourdet et al., 1997; Petit et al., 2007). Such polymers, like poly (N-isoprpylacrylamide) and poly (ethylene glycol) (PEG), with a character of lower critical solution temperature (LCST), were attached to the skeleton of the HPAM; then, the thermally triggered response of these polymers brought an increase of the viscosity and elastic modulus at temperatures above LCST (Chen et al., 2013; Sarsenbekuly et al., 2017b; Chen et al., 2020; Li et al., 2021). Moreover, the dynamic simulation demonstrated that the HPAM incorporated with PEG units should have larger viscosity and stronger salt tolerance at high temperature because the modified monomers with alkyl ether bonds bring a steric hindrance and will reduce the curliness of the molecule chains (Yao et al., 2012; Zhang et al., 2015). Meanwhile, the incorporation of HPAM by hydrophobic long-alkyl groups displayed enhanced temperature and salinity tolerance (Lai et al., 2013; Liu et al., 2013; Ye et al., 2014; Gou et al., 2015c; Sarsenbekuly et al., 2017a), the modified HPAM by hydrophilic sulfonate groups also exhibited relatively high viscosity at high salinity and temperature (Gou et al., 2014; Li et al., 2018; Zhang et al., 2018; Hu et al., 2019; Ji et al., 2020; Tchameni et al., 2020), and even the incorporated HPAM by both long-alkyl groups and sulfonate groups showed improved rheological properties and salt resistance (Yuan et al., 2013; Deng et al., 2014; Gou et al., 2015b), but these results were not sufficient to meet the viscosity requirements of the polymer fluids in the brines from high-temperature and high-salt reservoirs. In addition, the structures of β-cyclodextrin in the HPAM skeleton displayed better temperature and salt tolerance due to the hydrophobic associating effect (Liu et al., 2013; Wei et al., 2015; Pu et al., 2016; Zhang et al.,

2018; Peng et al., 2019), and some nature polysaccharides as flooding polymers were found to have a relatively low viscosity dependence on temperature and salinity (Gou et al., 2017; Liang et al., 2019), but the cost of polysaccharides, as well as β-cyclodextrin, limited their practice in the oil fields.
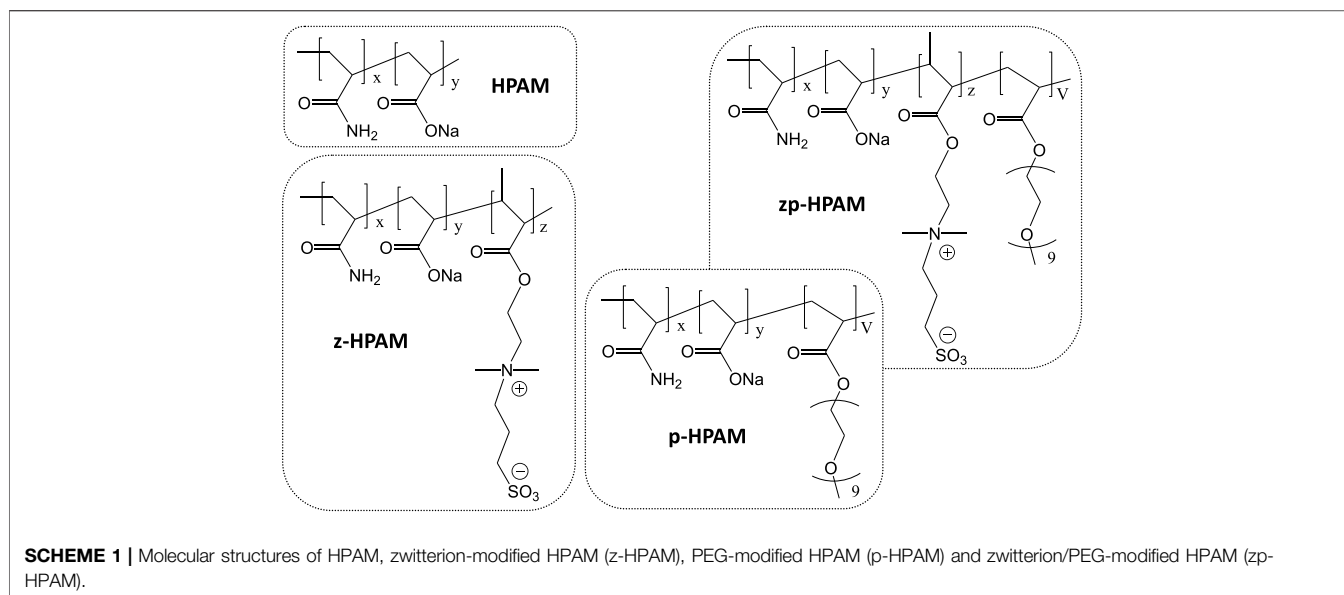
Zwitterionic polymers are composed of the main backbone chain and many side chains with positive and negative ions (Ladd et al., 2008). They are very hydrophilic because the solvation of zwitterions on the polymer chains can produce high solvent water retention and form a deeply hydrated layer around the polymer chains through anionic and cationic hydration (Leng et al., 2015). They also have strong salt affinity because the zwitterions on the polymer chains can electrostatically adsorb salt counterions in water (Li et al., 2020). So, zwitterionic polymers readily stretch in salt solution and have greater solubility in salt solution than in pure water (Mary et al., 2007), which is named as anti-polyelectrolyte behavior, i.e., "salting-in" effect (Yang et al., 2015; Xiao et al., 2018). Obviously, such superhydrophilicity and "salting-in" effect of zwitterionic polymers can reduce the dehydration of polymer chains at high temperatures, and thus can possibly overcome the "salting-out" effect of polymers under high salinity. Unfortunately, only little literature has focused on this topic for the enhanced oil recovery (Gou et al., 2015a; Dai et al., 2017; Liu et al., 2020). A modified HPAM with zwitterionic betaine groups and long alkyl groups reported by Kang et al. showed salt thickening behavior; a salt thickening mechanism was proposed that the destroyed inner salt bond of zwitterionic betaine groups in salt solution brought a greater hydrodynamic diameter of polymer molecules, and the inter-molecular hydrophobic interaction of the long alkyl groups in salt solution produced a stronger hydrophobic association (Zhu et al., 2017).

Herein, both zwitterionic sulfobetaine acrylate monomer and PEG-containing acrylate monomer were copolymerized with acrylamide (AM) and acrylic acid (AA) to prepare zwitterion-modified HPAM (z-HPAM), PEG-modified HPAM (p-HPAM), and zwitterion/PEG-modified HPAM (zp-HPAM) in order to study the rheological properties at different salinities and temperatures. The structures of these copolymers are shown in **Scheme 1**. It is found that zwitterionic sulfobetaine-unit incorporated HPAM (z-HPAM) obviously increases the viscosity under high salinity and high temperature, the incorporated HPAM with PEG units (p-HPAM) also exhibits enhanced salinity and temperature tolerance. The optimized zp-HPAM containing zwitterionic units and PEG units shows relatively high viscosity and good viscosity retention at 90°C in a synthetic brine of $20 \times 10^4$ mg/L salinity. The synergistic combination of zwitterionic units and PEG units in the zp-HPAM is considered to enhance the tolerance to high salinity and high temperature.

# EXPERIMENTAL

## Materials

Acrylamide (AM, 99%), acrylic acid (AA, >99%), and zwitterionic monomer [2-(Methacryloyloxy)ethyl]dimethyl-(3-sulfopropyl) ammonium inner salt (MDSA) were supplied by Shanghai Aladdin Biochemical Technology Co., Ltd., China.

**SCHEME 1 |** Molecular structures of HPAM, zwitterion-modified HPAM (z-HPAM), PEG-modified HPAM (p-HPAM) and zwitterion/PEG-modified HPAM (zp-HPAM).

Poly(ethylene glycol) monomethyl ether acrylate ($H_2C = CHCO_2(CH_2CH_2O)_nCH_3$, $n \approx 9$, PEGMA) was provided by Shanghai Xianding Biotechnology Co., Ltd. Potassium persulfate ($K_2S_2O_8$), NaOH, anhydrous alcohol, NaCl, $MgCl_2$, and $CaCl_2$ were purchased from Sinopharm Chemical Reagent Co., Ltd. All reagents were of analytical grade and used directly without further purification. All aqueous solutions were prepared using ultrapure water with a resistivity of 18.25 MΩ cm.

## Synthesis of Copolymers

For the copolymer synthesis, the total mass of AM and AA was fixed at 20 g, and a calculated volume of water was used to dilute the reactants to a monomer concentration of 10 wt%. In a typical process, a certain amount of AM, AA, and zwitterionic monomer MDSA were respectively dissolved in water, and the AA solution was then neutralized by isostoichiometric NaOH. All solutions were added to a 500-ml round-bottom three-necked flask, and a certain amount of PEGMA was added into the mixture. The monomers' molar ratio, namely, $n_{AM}:n_{AA}:n_{MDSA}:n_{PEGMA}$, was signed as x/y/z/V (x + y = 10) to label the sample. Next, the reaction solution was placed into a water bath at 70°C and bubbled with $N_2$ under stirring at least for 30 min to exclude dissolved oxygen. Subsequently, 10 ml of aqueous solution of potassium persulfate (0.57% of the total monomer mass) was added to the reaction mixture to initiate free radical polymerization. The reaction mixture was stirred under $N_2$ atmosphere for 3 h to form a viscous copolymer solution.

## Characterization

For the measurements of $^1H$ NMR spectroscopy and FT-IR spectroscopy, the copolymer samples were precipitated and washed with anhydrous ethanol to remove water, unreacted monomers, and initiator, followed by a drying under vacuum at 50°C for 10 h. $^1H$ NMR spectra were recorded on a Bruker AV 500 MHz spectrometer in $D_2O$ at 25°C. FT-IR spectra were measured on a Bruker Vertex 70 spectrometer according to the KBr-disk method between 4000 and 400 $cm^{-1}$. Morphology observation of the copolymer solutions was performed on a JSM-6700F scanning electron microscopy (SEM) with a voltage of 5.0 kV, in which the copolymer solutions (2.5wt%) were first dropped onto quartz sheets, quickly frozen in liquid nitrogen, and then freeze-dried before being coated with gold.
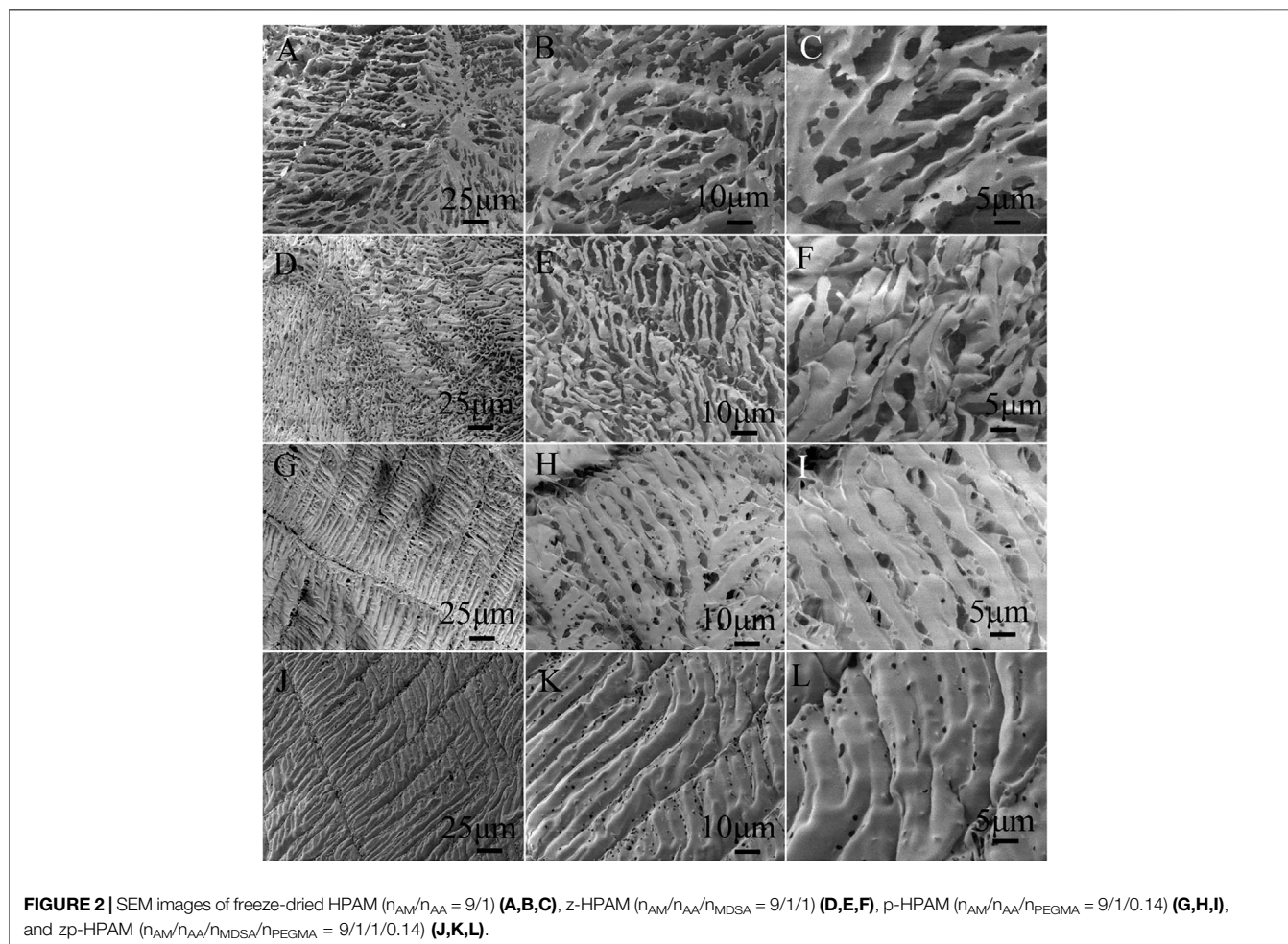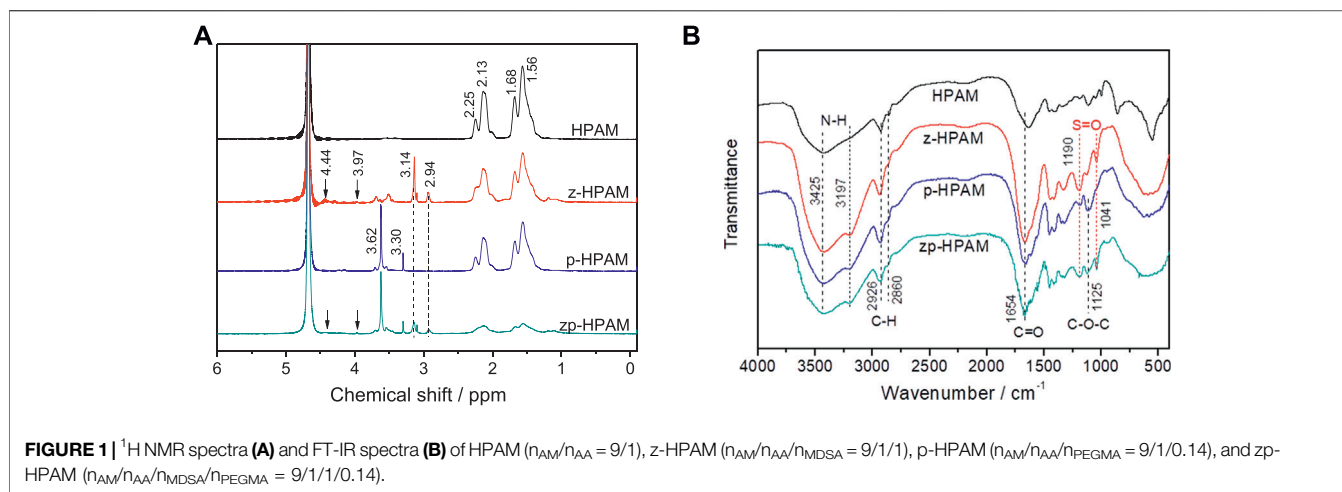
## Preparation of Salt Solutions and Viscosity Measurements

In order to prepare solutions for viscosity measurement, the as-obtained 10 wt% copolymer solution was diluted with water and continually stirred to obtain a homogeneous solution of 5 wt% copolymers. Then, different amounts of salts were dissolved in deionized water to prepare synthetic brines, in which the molar ratio of $Na^+/Ca^{2+}/Mg^{2+}$ was fixed at 25.3/1/1.6. Thereafter, 50 ml of copolymer solution (5 wt%) was mixed with 50 ml of synthetic brines to obtain a series of copolymer solutions with different salinities from $1 \times 10^4$ to $20 \times 10^4$ mg/L of the total dissolved solids (TDS). All viscosity measurements were carried out on a Rheolab QC (Anton Paar, Austria) rotational rheometer using CC39 concentric-cylinder testing cup between 25 and 90°C by ascending shear rate ramps from 0.1 to 100 $s^{-1}$. The shear viscosity at different temperature was recorded at a fixed shear rate of 100 $s^{-1}$.

# RESULTS AND DISCUSSION

## FT-IR and NMR Characterization

The free radical polymerization of AM, AA, sulfobetaine methacrylate, and poly(ethylene glycol) methacrylate was

**FIGURE 1 |** $^1$H NMR spectra **(A)** and FT-IR spectra **(B)** of HPAM ($n_{AM}/n_{AA}$ = 9/1), z-HPAM ($n_{AM}/n_{AA}/n_{MDSA}$ = 9/1/1), p-HPAM ($n_{AM}/n_{AA}/n_{PEGMA}$ = 9/1/0.14), and zp-HPAM ($n_{AM}/n_{AA}/n_{MDSA}/n_{PEGMA}$ = 9/1/1/0.14).



**FIGURE 2 |** SEM images of freeze-dried HPAM ($n_{AM}/n_{AA}$ = 9/1) **(A,B,C)**, z-HPAM ($n_{AM}/n_{AA}/n_{MDSA}$ = 9/1/1) **(D,E,F)**, p-HPAM ($n_{AM}/n_{AA}/n_{PEGMA}$ = 9/1/0.14) **(G,H,I)**, and zp-HPAM ($n_{AM}/n_{AA}/n_{MDSA}/n_{PEGMA}$ = 9/1/1/0.14) **(J,K,L)**.

initiated by commonly used potassium persulfate. The as-obtained copolymer samples of HPAM, zwitterion-modified HPAM (z-HPAM), PEG-modified HPAM (p-HPAM), and zwitterion/PEG-modified HPAM (zp-HPAM) were

characterized by $^1$H NMR spectra, as shown in **Figure 1A**. For all samples, the peak at 4.68 ppm is due to residue solvent water, while the peaks at 1.56, 1.68, 2.13, and 2.25 ppm are ascribed to the skeleton of acrylate and acrylamide. The characteristic peaks

at 4.44, 3.97, 3.14, and 2.94 ppm reveal the presence of zwitterionic sulfobetaine groups in the z-HPAM and the zp-HPAM (Chang et al., 2006; Han et al., 2013), while in the p-HPAM and the zp-HPAM, the peaks at 3.62 and 3.30 ppm correspond to the O-CH$_2$ and O-CH$_3$ unit of PEG, respectively. In the FT-IR spectra of these samples (**Figure 1B**), the typical peaks at 3,425 and 3,197 cm$^{-1}$ are attributed to N-H bonds, while those at 2,860 and 2,925 cm$^{-1}$ are ascribed to CH$_2$ groups, and that peak around 1,654 cm$^{-1}$ represents carbonyl groups in all samples. The characteristic peaks at 1,041 and 1,190 cm$^{-1}$ in the z-HPAM and the zp-HPAM are caused by the symmetric stretching vibration of sulfonate groups from the zwitterionic units (Zhao et al., 2010), while that broad peak at 1,125 cm$^{-1}$ in the p-HPAM and the zp-HPAM is evidence of C-O-C groups in the PEG units. All these results demonstrate that the designed copolymers have been successfully synthesized by the free radical polymerization.

## SEM Characterization

The freeze-dried samples of HPAM, z-HPAM, p-HPAM, and zp-HPAM solutions were observed by SEM to investigate the microscopic structure of these copolymers in solution, as shown in **Figure 2**. It is found that the HPAM sample (**Figures 2A–C**) shows an irregular spatial network, which should be attributed to the aggregation and entanglement caused by the hydrogen-bond interaction between the amide and carboxyl groups in the polymer chains. The z-HPAM sample (**Figures 2D–F**) displays a more compact network and the pore size in the network is significantly reduced; the reason should be ascribed to the additional intermolecular electrostatic crosslinking *via* the ion pairing of two zwitterionic groups attached on different polymer chains. However, an ordered structure can be found in the sample of p-HPAM (**Figures 2G–I**), which should be related with the "comb-like" structure of the PEGMA segments in the copolymer skeleton, because the additional hydrogen-bond interaction between the PEG units and amide groups in the p-HPAM sample can facilitate the formation of the ordered structure. Comparing **Figures 2G–I** and **Figure 2J–L**, the network structure of the later zp-HPAM sample is more ordered than that of the p-HPAM, and the pore size of the zp-HPAM network is much smaller than that of the p-HPAM, which may mean more crosslinking sites in the spatial structure. We think that such a dense and ordered structure reveals that the zp-HPAM chains have more spatial crosslinking sites in the solution, and thus forming more uniform spatial distribution.

In aqueous solution, the HPAM sample exhibits a loose spatial network through the hydrogen bonding interaction of the amide and carboxylate, but in the z-HPAM sample, the additional crosslinking effect from the zwitterionic units promotes a formation of a denser network structure. However, for p-HPAM and zp-HPAM samples, the presence of PEG units strengthens the hydrogen bonding interaction and promotes the association of polymer chains to form ordered structures. The enhanced hydrogen bonding by the PEG units and the electrostatic crosslinking by the zwitterionic units in the zp-HPAM sample help to form a more uniform and stable spatial

network, which will be beneficial to maintain the system viscosity under the harsh conditions.

## Viscosity of HPAM and Zwitterion-Modified HPAM

The homogeneous copolymer solutions with a concentration of 2.5 wt% were used to measure the rheology properties in pure water and the synthetic brines, and the apparent viscosity of these solutions was recorded at the fixed shear rate of 100 s$^{-1}$. **Figure 3A** shows the apparent viscosity change of the HPAM and the z-HPAM at 25°C under different salinity. It is found that the viscosity of the HPAM rapidly drops from 105 mPa s to 70 mPa s when the salinity exceeds 1 × 10$^4$ mg/L. However, after adding 10% MDSA to AM/AA in copolymerization, the obtained z-HPAM is found to be more viscous than the HPAM, with a viscosity value between 140 and 190 mPa s. It is worth noting that changing the AM/AA molar ratio from 9/1 to 9.5/0.5 has little effect on the solution viscosity at different salinities. The viscosity of the z-HPAM solution decreases first and then gradually increases with the salinity increasing. The final viscosity under the highest salinity (20 × 10$^4$ mg/L) is similar to that value in pure water, which is better than the sufitiobetaine-modified HPAM as reported by Gou et al. (2015a). The salt thickening of the z-HPAM under high salinity can be ascribed to the following possible reasons: (1) The "salting-in" effect of zwitterionic units can overcome the viscosity reduction of the HPAM skeleton by the "salting-out" effect (Mary et al., 2007; Yang et al., 2015; Xiao et al., 2018; Li et al., 2020). The modified HPAM with zwitterionic betaine groups were found to have a larger hydrodynamic diameter in salt solution than in pure water, because the better solubility of zwitterionic betaine groups in salt solution can partially offset the coiling of polymer chains (Zhu et al., 2017). (2) The intermolecular ion pairing of the zwitterionic ions attached on different polymer chains can generate electrostatic crosslinking sites between different polymer chains. (3) The intermolecular crosslinking sites can be formed by the bridging of the divalent cations (Ca$^{2+}$ and Mg$^{2+}$) in the synthetic brine (Zhu et al., 2017; Bai et al., 2021). **Figure 3B** shows the change in the viscosity of the z-HPAM (n$_{AM}$/n$_{AA}$/n$_{MDSA}$ = 9/1/1) with respect to salinity at different temperatures. The viscosity in the highest salinity solution is found to be approximately 70% of that value in pure water between 35°C and 75°C, whereas at 90°C, the viscosity value increases under higher salinities. Interestingly, the viscosity value at 90°C under 20 × 10$^4$ mg/L salinity reaches 42.8 mPa s, which is about 1.6 times the value at 90°C in pure water.

**Figures 3C,D** show the viscosity change of the HPAM (n$_{AM}$/n$_{AA}$ = 9/1) and the z-HPAM (n$_{AM}$/n$_{AA}$/n$_{MDSA}$ = 9/1/1) with temperature at different salinities. It is clear that the viscosity of HPAM in pure water or in the synthetic brines gradually decreases to about 10 mPa s as the temperature rises to 90°C (**Figure 3C**), and the viscosity retention rate at 90°C changes in a range of 10.7%–13.8% of the corresponding value at 25°C under different salinities. The viscosity under the harsh condition (i.e., 90°C, 20 × 10$^4$ mg/L salinity, the same below) only retains 9.6% of the value under the normal condition
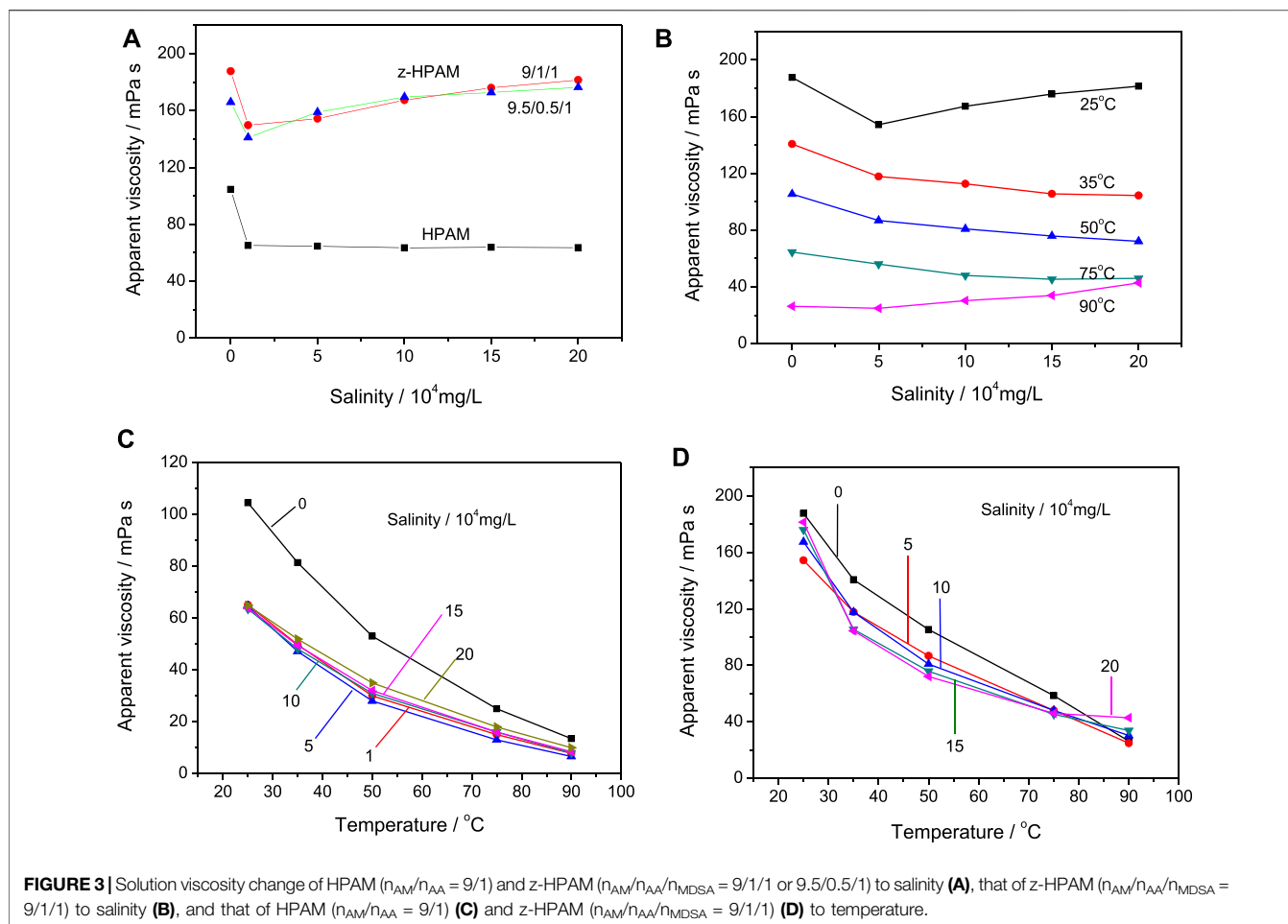
**FIGURE 3 |** Solution viscosity change of HPAM ($n_{AM}/n_{AA}$ = 9/1) and z-HPAM ($n_{AM}/n_{AA}/n_{MDSA}$ = 9/1/1 or 9.5/0.5/1) to salinity **(A)**, that of z-HPAM ($n_{AM}/n_{AA}/n_{MDSA}$ = 9/1/1) to salinity **(B)**, and that of HPAM ($n_{AM}/n_{AA}$ = 9/1) **(C)** and z-HPAM ($n_{AM}/n_{AA}/n_{MDSA}$ = 9/1/1) **(D)** to temperature.

**TABLE 1 |** Viscosity (mPa·s) of HPAM and zwitterion-modified HPAM at 90°C.

| Components ($n_{AM}/n_{AA}/n_{MDSA}$) | Salinity/$10^4$ mg/L | | | | | |
|---|---|---|---|---|---|---|
|  | 0 | 1 | 5 | 10 | 15 | 20 |
| 9/1/1 | 26.3 | — | 24.9 | 30.3 | 33.8 | 42.8 |
| 9/1/0.5 | 18.5 | 10.9 | — | 11.1 | — | 11.7 |
| 9/1/0.25 | 8.7 | 4.1 | — | 5.6 | — | 7.5 |
| 9/1/0 | 13.5 | 7.8 | 6.6 | 7.9 | 8.4 | 10.0 |

(i.e., 25°C in pure water, the same below). For the z-HPAM sample (**Figure 3D**), the viscosity data similarly show a decrease with increasing temperature. From 35°C to 75°C, the viscosity of the z-HPAM at higher salinities (10–20 × $10^4$ mg/L) is lower than that at lower salinity cases (0–5 × $10^4$ mg/L), but at 90°C, the viscosity at the highest salinity is greater than that of low salinity. The viscosity retention rate at 90°C gradually increases from 14.1% to 23.6% of the value at 25°C under different salinities from 0 to 20 × $10^4$ mg/L. Such viscosity retention values of the z-HPAM at 90°C are much larger than those of the HPAM at 90°C, indicating an enhanced tolerance to high temperature under the harsh condition. In addition, the viscosity retention rate under the harsh condition is 22.9% of that under the normal condition.

**Table 1** shows the viscosity data of the z-HPAM with different zwitterion content at 90°C under different salinities. Obviously, the viscosity of z-HPAM decreases first and then increases at different salinities, which should be attributed to the "salting-in" and "electrostatic crosslinking" effects of zwitterionic units (Li et al., 2020). Noticeably, the viscosity value obviously decreases at any salinity when the zwitterion content is reduced. When the zwitterion content is 5% relative to AM/AA ($n_{AM}/n_{AA}/n_{MDSA}$ = 9/1/0.5), the z-HPAM sample shows viscosity values similar to those of the HPAM, and when the zwitterion content is 10% ($n_{AM}/n_{AA}/n_{MDSA}$ = 9/1/1), the viscosity is much larger than that of the HPAM. Therefore, we think the content of 10% zwitterionic monomer to AM/AA ($n_{AM}/n_{AA}/n_{MDSA}$ = 9/1/1) is effective for enhancing viscosity under high salinities, and the presence of zwitterionic units can also improve the tolerance to high temperature.

## Viscosity of PEG-Modified HPAM

The polymers of PEG-containing acrylates were reported to have a thermally triggered response to temperature rising (Han et al., 2003; Ali and Stöver, 2004; Li et al., 2007), and the dynamic simulation demonstrated that the HPAM incorporated with PEG-containing units should have higher viscosity and stronger salt resistance (Yao et al., 2012; Zhang et al., 2015). In this work, poly(ethylene glycol) monomethyl ether acrylate

**FIGURE 4** | Solution viscosity change of p-HPAM ($n_{AM}/n_{AA/PEGMA}$ = 9/1/0.14) **(A)** and ($n_{AM}/n_{AA/PEGMA}$ = 9/1/0.12) **(B)** to salinity at different temperature.
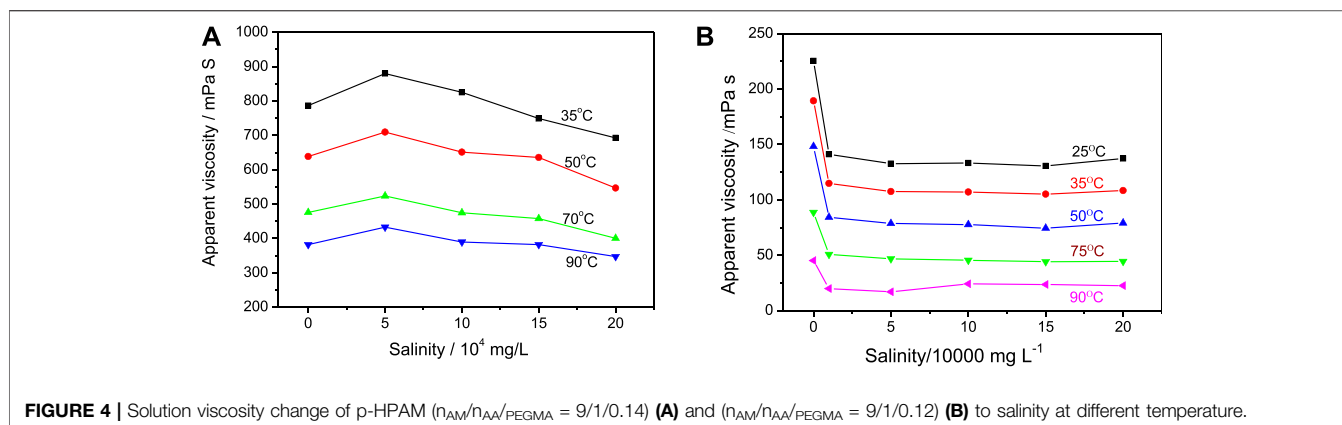
(PEGMA) with a long PEG tail was used to modify HPAM. It was found that the viscosity of the synthesis solution was greatly increased when adding PEGMA in the copolymerization. When the molar content of PEGMA to AM/AA reached 2.0%, the resulting p-HPAM solution after the polymerization reaction showed typical viscoelasticity, and it was difficult to obtain a homogenous copolymer solution through diluting and stirring. In our experiment, a relatively homogenous solution of the p-HPAM was obtained when the PEGMA content was 1.4% (i.e., $n_{AM}/n_{AA}/n_{PEGMA}$ = 9/1/0.14). The rheological results of this p-HPAM sample are shown in **Figure 4A**. The viscosity values at different conditions are relatively large, ranging from 350 to 880 mPa s. As the salinity increases, the sample viscosity increases at $5 \times 10^4$ mg/L salinity, but gradually decreases when the salinity increases from $10 \times 10^4$ to $20 \times 10^4$ mg/L. The viscosity values at the highest salinity are about 80%–90% of those values in pure water at a same temperature. From another view, the viscosity data can be rearranged according to the temperature change (Supporting information, **Supplementary Figure S1A**). It is found that the p-HPAM solution at any salinity shows a viscosity decrease with increasing temperature. Under the same salinity, the viscosity values at 90°C (between 347 and 433 mPa s) are about half of the values at 35°C (between 693 and 787 mPa s). The viscosity retention under $20 \times 10^4$ mg/L salinity at 90°C is about 44% of the value in pure water at 35°C.
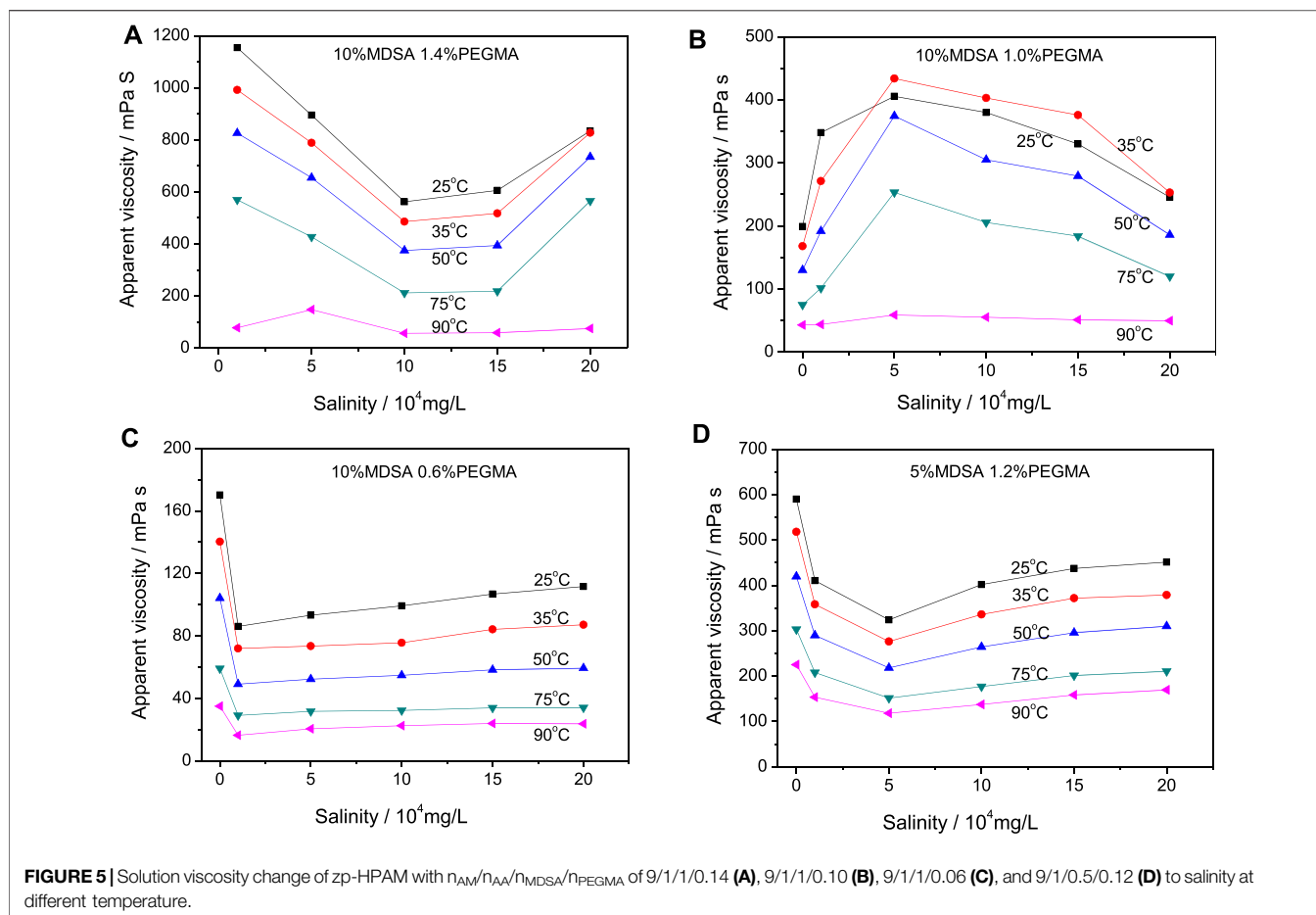
In addition, another p-HPAM sample with a lower PEGMA content ($n_{AM}/n_{AA}/n_{PEGMA}$ = 9/1/0.12) was prepared and characterized by the rheological properties. The solution viscosity values to salinity change are shown in **Figure 4B** (the rearranged data to temperature change are shown in **Supplementary Figure S1B**). The viscosity of this sample ranges from 20 to 225 mPa s under all measurement conditions, which is obviously smaller than those of the last p-HPAM sample. The viscosity retention rate of this sample under the harsh condition is only 16% of the value in pure water at 35°C and only 10% of the value in pure water at 25°C. Thus, the PEGMA content in the p-HPAM shows a great influence on the viscosity of the sample and its tolerance to the environmental salinity and temperature. Moreover, based on the comparison of **Figures 4A,B**, the p-HPAM ($n_{AM}/n_{AA}/n_{PEGMA}$ = 9/1/0.14) has better salinity tolerance

than the sample with lower PEGMA ($n_{AM}/n_{AA}/n_{PEGMA}$ = 9/1/0.12).

## Viscosity of Zwitterion/PEG-Modified HPAM

Zwitterion-modified HPAM (z-HPAM) is found to have better rheological properties at high salinity and high temperature than the unmodified HPAM. Similarly, the modified HPAM by PEG units (p-HPAM) exhibits better viscosity retention than the unmodified HPAM at high salinity and high temperature. If both zwitterionic units and PEG units are incorporated into the HPAM skeleton together, we believe that the obtained zwitterion/PEG-modified HPAM (zp-HPAM) may have a synergistic effect on the rheological properties at high salinity and high temperature. Therefore, the zp-HPAM samples were prepared, in which the molar amount of MSDA relative to AM/AA was fixed at 10% and that of PEGMA was 1.4%, 1.0%, and 0.6% for comparison. The viscosity data of these samples are plotted with salinity change (**Figures 5A–C**) and temperature change (**Supplementary Figures S2A–C**), respectively. For the sample containing 1.4% PEGMA, the measured viscosity varies from 70 to 1,200 mPa s under all measurement conditions. When the temperature rises from 25°C to 75°C (**Figure 5A**), the solution viscosity first decreases along with the salinity increase until the salinity reaches $10 \times 10^4$ mg/L; then, as the salinity rises from $10 \times 10^4$ mg/L to $20 \times 10^4$ mg/L, the solution viscosity increases instead. The viscosity at $20 \times 10^4$ mg/L salinity maintains more than 70% retention of the value in pure water at a same temperature. However, at 90°C, the solution viscosity is relatively stable under different salinities. Moreover, it is clear that the solution viscosity obviously decreases with the temperature increasing from 25°C to 90°C (**Supplementary Figure S2A**). The viscosity curve at low salinity ($1 \times 10^4$ mg/L and $5 \times 10^4$ mg/L) or the highest salinity ($20 \times 10^4$ mg/L) is above the viscosity curve at middle salinity ($10 \times 10^4$ mg/L and $15 \times 10^4$ mg/L), which indicates that the sample solution has a lower viscosity under the middle salinity.

For the sample with 1.0% PEGMA, the viscosity value varies between 30 and 430 mPa s under all measurement conditions (**Figure 5B**), which is obviously lower than the last sample.

**FIGURE 5** | Solution viscosity change of zp-HPAM with $n_{AM}/n_{AA}/n_{MDSA}/n_{PEGMA}$ of 9/1/1/0.14 **(A)**, 9/1/1/0.10 **(B)**, 9/1/1/0.06 **(C)**, and 9/1/0.5/0.12 **(D)** to salinity at different temperature.

Interestingly, under low salinity from 0 to $5 \times 10^4$ mg/L, the sample viscosity gradually increases. Then, with the salinity rising from $10 \times 10^4$ mg/L to $20 \times 10^4$ mg/L, the sample viscosity decreases in turn. Noticeably, at any same temperature, the viscosity of the sample under $20 \times 10^4$ mg/L is greater than that in pure water. Moreover, the sample in pure water or under a salinity of $1 \times 10^4$ mg/L shows a gradual decrease in viscosity from 25 to 90°C (**Supplementary Figure S2B**). However, as the salinity is above $5 \times 10^4$ mg/L, the sample viscosity increases first between 25°C and 35°C, and then decreases between 35°C and 90°C. It is also noticeable that the viscosity curves under the middle salinity (from $5 \times 10^4$ mg/L to $15 \times 10^4$ mg/L) are above those under other salinity cases (0, $1 \times 10^4$ mg/L and $20 \times 10^4$ mg/L). The final viscosity under the harsh condition is 39.7 mPa s, a 20% retention rate of the value under the normal condition.

**Figure 5C** and **Supplementary Figure S2C** show the viscosity data of the sample with 0.6% PEGMA. It is found that the measured solution viscosity varies between 16.5 and 170 mPa s, which is lower than the last two samples. In pure water, the sample solution viscosity varies between 170.2 and 35.1 mPa s at different temperatures (**Figure 5C**), but when the salinity reaches $1 \times 10^4$ mg/L, the viscosity drops sharply to about a half of that in pure water. Then, as the salinity increases, the solution viscosity slowly increases. When the salinity

reaches $20 \times 10^4$ mg/L, the viscosity is about 60% of that in pure water at the same temperature. Moreover, the solution viscosity gradually decreases with increasing temperature under all salinities (**Supplementary Figure S2C**). The final viscosity under the harsh condition remains only 12% of that under the normal condition.

Comparing the curves in **Figures 5A,B**, the sample with 1.4% PEGMA has a higher viscosity in pure water, and the viscosity change shows concave curves with the increase of the salinity (**Figure 5A**), whereas the sample with 1.0% PEGMA has a lower viscosity in pure water, and the viscosity change shows convex curves with the salinity increasing (**Figure 5B**). Considering that the high viscosity of the sample with 1.4% PEGMA under low salinity will cause difficulty for fluid pumping in practices, the sample with 1.0% PEGMA is considered as the best one. Moreover, all three samples show a basic downward trend with the temperature increasing (**Supplementary Figures S2A–C**), but the viscosity of the zp-HPAM samples with 1.4 and 1.0% PEGMA drops sharply when the temperature increases from 75 to 90°C, which implies rapidly lowered viscosity tolerance at 90°C. Obviously, the significant difference in the salinity and temperature resistance of these zp-HPAM samples should be attributed to the different PEGMA content,

which will seriously affect the synergistic interaction of the zwitterion units and the PEG units.

It should be noted that the lowered tolerance of the zp-HPAM samples at 90°C (**Supplementary Figures S2A,B**) should be ascribed to the presence of the zwitterionic units because the p-HPAM samples (**Supplementary Figures S1A,B**) have exhibited relatively good environment tolerance at 90°C. So, we think that the environmental tolerance of the zp-HPAM at 90°C may be improved if lowering the zwitterion content. Therefore, the ratio of $n_{AM}/n_{AA}/n_{MDSA}/n_{PEGMA}$ in a new zp-HPAM sample was optimized to be 9/1/0.5/0.12. **Figure 5D** and **Supplementary Figure S2D** show the rheological properties of this zp-HPAM sample. At any temperature, the viscosity decreases first and then increases with the salinity increasing (**Figure 5D**) and the corresponding viscosity retentions under $20 \times 10^4$ mg/L salinity rise to 53%–73% of those values in pure water. In pure water, the sample viscosity retention at 90°C is about 38% of that value at 25°C (**Supplementary Figure S2D**), which is comparable with the hydrophobically associating polyacrylamide under similar conditions (Zheng and Huang, 2019). Though the viscosity of the sample in the synthetic brines gradually decreases with the temperature increasing, the final viscosity at the harsh condition remains 170 mPa s, a 29% retention of the value under the normal condition. This retention rate can be considered as a significant value for the HPAM-based fluid systems under the harsh condition.

## CONCLUSION

The copolymers of HPAM, zwitterion-modified HPAM (z-HPAM), PEG-modified HPAM, and zwitterion/PEG-modified HPAM (zp-HPAM) were prepared by the free radical polymerization. The rheological properties of these copolymers in the aqueous solutions were studied under different salinities and temperatures. The following points were mainly concluded: (1) The viscosity of the HPAM under the harsh condition was only 9.6% of the value under the normal condition, while the z-HPAM significantly enhanced the viscosity retention to 22.9% under the harsh condition due to the salting-in effect and the electrostatic crosslinking by the divalent cations and the zwitterion units. (2) The PEG units in the p-HPAM samples improved the salinity and temperature resistances because they could strengthen the hydrogen bonding between the polymer chains and form a spatially ordered structure. (3) The zp-HPAM samples with the zwitterion and PEG units showed a complex impact on the rheological properties, the optimized zp-HPAM sample under the harsh condition exhibited a viscosity value of 170 mPa s and a viscosity retention rate up to 29% of the value under the normal condition. The good salinity and temperature tolerances of the zp-HPAM samples should be attributed to the synergistic effects of the zwitterion and PEG units. The enhanced rheological properties of the zp-HPAM under the harsh condition should be significant for the enhanced oil recovery in the water-soluble polymer flooding.

## DATA AVAILABILITY STATEMENT

The original contributions presented in the study are included in the article/**Supplementary Material**. Further inquiries can be directed to the corresponding authors.

## AUTHOR CONTRIBUTIONS

DL, GL, and JZ contributed to the conception and design of the study. SL, YC, YW, and CL performed the data collection and software treatment. GL and JZ performed the data analysis. DL gave a draft of the manuscript. GL, JZ, and DL wrote sections of the manuscript. All authors contributed to manuscript revision, read, and approved the submitted version.

## SUPPLEMENTARY MATERIAL

The Supplementary Material for this article can be found online at: https://www.frontiersin.org/articles/10.3389/fmats.2021.788746/full#supplementary-material

## REFERENCES

Abidin, A. Z., Puspasari, T., and Nugroho, W. A. (2012). Polymers for Enhanced Oil Recovery Technology. *Proced. Chem.* 4, 11–16. doi:10.1016/j.proche.2012.06.002

Ali, M. M., and Stöver, H. D. H. (2004). Well-Defined Amphiphilic Thermosensitive Copolymers Based on Poly(ethylene Glycol) Monomethacrylate) and Methyl Methacrylate Prepared by Atom Transfer Radical Polymerization. *Macromolecules* 37 (14), 5219–5227. doi:10.1021/ma030485m

Bai, J., Wang, R., Ju, M., Zhou, J., Zhang, L., and Jiao, T. (2021). Facile Preparation and High Performance of Wearable Strain Sensors Based on Ionically Cross-Linked Composite Hydrogels. *Sci. China Mater.* 64 (4), 942–952. doi:10.1007/s40843-020-1507-0

Chang, Y., Chen, S., Zhang, Z., and Jiang, S. (2006). Highly Protein-Resistant Coatings from Well-Defined Diblock Copolymers Containing Sulfobetaines. *Langmuir* 22 (5), 2222–2226. doi:10.1021/la052962v

Chen, H., Liu, H., Zhang, S., and Feng, Y. (2020). Smart Thermoviscosifying Polymer for Improving Drag Reduction in Slick-Water Hydrofracking. *Fuel* 278, 118408. doi:10.1016/j.fuel.2020.118408

Chen, Q., Wang, Y., Lu, Z., and Feng, Y. (2013). Thermoviscosifying Polymer Used for Enhanced Oil Recovery: Rheological Behaviors and Core Flooding Test. *Polym. Bull.* 70 (2), 391–401. doi:10.1007/s00289-012-0798-7

Dai, C., Xu, Z., Wu, Y., Zou, C., Wu, X., Wang, T., et al. (2017). Design and Study of a Novel Thermal-Resistant and Shear-Stable Amphoteric Polyacrylamide in High-Salinity Solution. *Polymers* 9 (7), 296. doi:10.3390/polym9070296

Deng, Q., Li, H., Li, Y., Cao, X., Yang, Y., and Song, X. (2014). Rheological Properties and Salt Resistance of a Hydrophobically Associating Polyacrylamide. *Aust. J. Chem.* 67 (10), 1396–1402. doi:10.1071/ch14204

Gou, S., He, Y., Ma, Y., Luo, S., Zhang, Q., Jing, D., et al. (2015a). A Water-Soluble Antimicrobial Acrylamide Copolymer Containing Sulfitobetaine for Enhanced Oil Recovery. *RSC Adv.* 5 (64), 51549–51558. doi:10.1039/c5ra07495a

Gou, S., He, Y., Zhou, L., Zhao, P., Zhang, Q., Li, S., et al. (2015b). An Anti-biodegradable Hydrophobic Sulfonate-Based Acrylamide Copolymer

Containing 2,4-dichlorophenoxy for Enhanced Oil Recovery. *New J. Chem.* 39 (12), 9265–9274. doi:10.1039/c5nj01821h

Gou, S., Li, S., Feng, M., Zhang, Q., Pan, Q., Wen, J., et al. (2017). Novel Biodegradable Graft-Modified Water-Soluble Copolymer Using Acrylamide and Konjac Glucomannan for Enhanced Oil Recovery. *Ind. Eng. Chem. Res.* 56 (4), 942–951. doi:10.1021/acs.iecr.6b04649

Gou, S., Liu, M., Ye, Z., Zhou, L., Jiang, W., Cai, X., et al. (2014). Modification of a Nicotinic Acid Functionalized Water-Soluble Acrylamide Sulfonate Copolymer for Chemically Enhanced Oil Recovery. *J. Appl. Polym. Sci.* 131 (8), a–n. doi:10.1002/app.40166

Gou, S., Luo, S., Liu, T., Zhao, P., He, Y., Pan, Q., et al. (2015c). A Novel Water-Soluble Hydrophobically Associating Polyacrylamide Based on Oleic Imidazoline and Sulfonate for Enhanced Oil Recovery. *New J. Chem.* 39 (10), 7805–7814. doi:10.1039/c5nj01153a

Han, D., Letteri, R., Chan-Seng, D., Emrick, T., and Tu, H. (2013). Examination of Zwitterionic Polymers and Gels Subjected to Mechanical Constraints. *Polymer* 54 (12), 2887–2894. doi:10.1016/j.polymer.2013.04.003

Han, S., Hagiwara, M., and Ishizone, T. (2003). Synthesis of Thermally Sensitive Water-Soluble Polymethacrylates by Living Anionic Polymerizations of Oligo(ethylene Glycol) Methyl Ether Methacrylates. *Macromolecules* 36 (22), 8312–8319. doi:10.1021/ma0347971

Hourdet, D., L'Alloret, F., and Audebert, R. (1997). Synthesis of Thermoassociative Copolymers. *Polymer* 38 (10), 2535–2547. doi:10.1016/S0032-3861(96)00808-7

Hu, X., Ke, Y., Zhao, Y., Lu, S., Deng, Q., Yu, C., et al. (2019). Synthesis, Characterization and Solution Properties of β-cyclodextrin-functionalized Polyacrylamide/montmorillonite Nanocomposites. *Colloids Surf. A: Physicochemical Eng. Aspects* 560, 336–343. doi:10.1016/j.colsurfa.2018.10.035

Ji, Y. F., Cao, X. L., Zhu, Y. W., Xu, H., Sun, X. Z., and Li, H. T. (2020). Synthesis Of Super High Molecular Weight Copolymer Of AM/Naa/AMPS By Oxidation-Reduction And Controlled Radical Polymerization. *Pet. Sci.* 17 (1), 242–254. doi:10.1007/s12182-019-00385-1

Kamal, M. S., Sultan, A. S., Al-Mubaiyedh, U. A., and Hussein, I. A. (2015). Review on Polymer Flooding: Rheology, Adsorption, Stability, and Field Applications of Various Polymer Systems. *Polym. Rev.* 55 (3), 491–530. doi:10.1080/15583724.2014.982821

L'Alloret, F., Hourdet, D., and Audebert, R. (1995). Aqueous Solution Behavior of New Thermoassociative Polymers. *Colloid Polym. Sci.* 273 (12), 1163–1173. doi:10.1007/BF00653085

Ladd, J., Zhang, Z., Chen, S., Hower, J. C., and Jiang, S. (2008). Zwitterionic Polymers Exhibiting High Resistance to Nonspecific Protein Adsorption from Human Serum and Plasma. *Biomacromolecules* 9 (5), 1357–1361. doi:10.1021/bm701301s

Lai, N., Dong, W., Ye, Z., Dong, J., Qin, X., Chen, W., et al. (2013). A Water-Soluble Acrylamide Hydrophobically Associating Polymer: Synthesis, Characterization, and Properties as EOR Chemical. *J. Appl. Polym. Sci.* 129 (4), 1888–1896. doi:10.1002/app.38893

Leng, C., Hung, H.-C., Sun, S., Wang, D., Li, Y., Jiang, S., et al. (2015). Probing the Surface Hydration of Nonfouling Zwitterionic and PEG Materials in Contact with Proteins. *ACS Appl. Mater. Inter.* 7 (30), 16881–16888. doi:10.1021/acsami.5b05627

Li, D., Cui, Y., Wang, K., He, Q., Yan, X., and Li, J. (2007). Thermosensitive Nanostructures Comprising Gold Nanoparticles Grafted with Block Copolymers. *Adv. Funct. Mater.* 17 (16), 3134–3140. doi:10.1002/adfm.200700427

Li, D., Wei, Q., Wu, C., Zhang, X., Xue, Q., Zheng, T., et al. (2020). Superhydrophilicity and strong Salt-Affinity: Zwitterionic Polymer Grafted Surfaces with Significant Potentials Particularly in Biological Systems. *Adv. Colloid Interf. Sci.* 278, 102141. doi:10.1016/j.cis.2020.102141

Li, F., Zhu, W.-x., Yu, D.-z., Song, H., and Wang, K.-l. (2018). Rheological Properties and Enhanced Oil Recovery Performance of a Novel Sulfonate Polyacrylamide. *J. Macromolecular Sci. A* 55 (6), 449–454. doi:10.1080/10601325.2018.1470462

Li, S., Braun, O., Lauber, L., Leblanc, T., Su, X., and Feng, Y. (2021). Enhancing Oil Recovery from High-Temperature and High-Salinity Reservoirs with Smart Thermoviscosifying Polymers: A Laboratory Study. *Fuel* 288, 119777. doi:10.1016/j.fuel.2020.119777

Liang, K., Han, P., Chen, Q., Su, X., and Feng, Y. (2019). Comparative Study on Enhancing Oil Recovery under High Temperature and High Salinity: Polysaccharides versus Synthetic Polymer. *ACS Omega* 4 (6), 10620–10628. doi:10.1021/acsomega.9b00717

Liu, L., Gou, S., Zhang, H., Zhou, L., Tang, L., and Liu, L. (2020). A Zwitterionic Polymer Containing a Hydrophobic Group: Enhanced Rheological Properties. *New J. Chem.* 44 (23), 9703–9711. doi:10.1039/d0nj01687j

Liu, X., Jiang, W., Gou, S., Ye, Z., Feng, M., Lai, N., et al. (2013). Synthesis and Evaluation of Novel Water-Soluble Copolymers Based on Acrylamide and Modular β-cyclodextrin. *Carbohydr. Polym.* 96 (1), 47–56. doi:10.1016/j.carbpol.2013.03.053

Mary, P., Bendejacq, D. D., Labeau, M.-P., and Dupuis, P. (2007). Reconciling Low- and High-Salt Solution Behavior of Sulfobetaine Polyzwitterions. *J. Phys. Chem. B* 111 (27), 7767–7777. doi:10.1021/jp071995b

Peng, Z., Gou, S., Wu, Q., Zhou, L., Zhang, H., and Fei, Y. (2019). Modified Acrylamide Copolymers Based on β-cyclodextrin and Twin-Tail Structures for Enhanced Oil Recovery through Host-Guest Interactions. *New J. Chem.* 43 (14), 5363–5373. doi:10.1039/c8nj06432f

Peng, S., and Wu, C. (1999). Light Scattering Study of the Formation and Structure of Partially Hydrolyzed Poly(acrylamide)/Calcium(II) Complexes. *Macromolecules* 32 (3), 585–589. doi:10.1021/ma9809031

Petit, L., Karakasyan, C., Pantoustier, N., and Hourdet, D. (2007). Synthesis of Graft Polyacrylamide with Responsive Self-Assembling Properties in Aqueous media. *Polymer* 48 (24), 7098–7112. doi:10.1016/j.polymer.2007.09.040

Pu, W., Du, D., Liu, R., Li, K., and Huang, T. (2016). Synthesis and Evaluation of β-cyclodextrin-functionalized Hydrophobically Associating Polyacrylamide. *RSC Adv.* 6 (98), 96006–96014. doi:10.1039/c6ra14209e

Sarsenbekuly, B., Kang, W., Fan, H., Yang, H., Dai, C., Zhao, B., et al. (2017a). Study of Salt Tolerance and Temperature Resistance of a Hydrophobically Modified Polyacrylamide Based Novel Functional Polymer for EOR. *Colloids Surf. A: Physicochemical Eng. Aspects* 514, 91–97. doi:10.1016/j.colsurfa.2016.10.051

Sarsenbekuly, B., Kang, W., Yang, H., Zhao, B., Aidarova, S., Yu, B., et al. (2017b). Evaluation of Rheological Properties of a Novel Thermo-Viscosifying Functional Polymer for Enhanced Oil Recovery. *Colloids Surf. A: Physicochemical Eng. Aspects* 532, 405–410. doi:10.1016/j.colsurfa.2017.04.053

Tchameni, A. P., Xie, B., Zhang, H., Zhao, L., Luo, M., and Wen, J. (2020). Thermo-associating Polymers Based on Cross-Linked 2-Acrylamido-Methylpropane Sulfonic Acid, Part A: Synthesis and Solution Behavior. *Colloids Surf. A: Physicochemical Eng. Aspects* 593, 124611. doi:10.1016/j.colsurfa.2020.124611

Wang, Z. M., Song, G.-L., and Zhang, J. (2019). Corrosion Control in CO2 Enhanced Oil Recovery from a Perspective of Multiphase Fluids. *Front. Mater.* 6, 272. doi:10.3389/fmats.2019.00272

Wei, B., Romero-Zerón, L., and Rodrigue, D. (2015). Improved Viscoelasticity of Xanthan Gum through Self-Association with Surfactant: β-cyclodextrin Inclusion Complexes for Applications in Enhanced Oil Recovery. *Polym. Eng. Sci.* 55 (3), 523–532. doi:10.1002/pen.23912

Wever, D. A. Z., Picchioni, F., and Broekhuis, A. A. (2011). Polymers for Enhanced Oil Recovery: A Paradigm for Structure-Property Relationship in Aqueous Solution. *Prog. Polym. Sci.* 36 (11), 1558–1628. doi:10.1016/j.progpolymsci.2011.05.006

Xiao, S., Ren, B., Huang, L., Shen, M., Zhang, Y., Zhong, M., et al. (2018). Salt-responsive Zwitterionic Polymer Brushes with Anti-polyelectrolyte Property. *Curr. Opin. Chem. Eng.* 19, 86–93. doi:10.1016/j.coche.2017.12.008

Yang, J., Chen, H., Xiao, S., Shen, M., Chen, F., Fan, P., et al. (2015). Salt-Responsive Zwitterionic Polymer Brushes with Tunable Friction and Antifouling Properties. *Langmuir* 31 (33), 9125–9133. doi:10.1021/acs.langmuir.5b02119

Yao, L., Chen, P., Ding, B., Luo, J., Jiang, B., and Zhou, G. (2012). Molecular Design of Modified Polyacrylamide for the Salt Tolerance. *J. Mol. Model.* 18 (9), 4529–4545. doi:10.1007/s00894-012-1447-7

Ye, Z., Zhang, X., Chen, H., Han, L., Lv, C., Su, Z., et al. (2014). Synthesis and Characterization of an Associative Polymer with an Octylphenyl Polyoxyethylene Side Chain as a Potential Enhanced-Oil-Recovery Chemical. *J. Appl. Polym. Sci.* 131 (20). doi:10.1002/app.41024

Yuan, R., Li, Y., Li, C., Fang, H., and Wang, W. (2013). Study about How the Metal Cationic Ions Affect the Properties of Partially Hydrolyzed Hydrophobically Modified Polyacrylamide (HMHPAM) in Aqueous Solution. *Colloids Surf. A: Physicochemical Eng. Aspects* 434, 16–24. doi:10.1016/j.colsurfa.2013.05.036

Zhang, C., Wang, P., and Song, G. (2018). Performance Evaluation of STARPAM Polymer and Application in High Temperature and Salinity Reservoir. *Int. J. Anal. Chem.* 2018, 1–13. doi:10.1155/2018/9653953

Zhang, P., Yao, L., Luo, J.-h., Ding, B., Zhou, G., and Jiang, B. (2015). Dynamics Simulation on the Associative Properties of Amphiphilic Functional Monomer Modified Polyacrylamide Copolymers. *Chin. J. Polym. Sci.* 33 (4), 540–553. doi:10.1007/s10118-015-1605-3

Zhao, Y.-H., Wee, K.-H., and Bai, R. (2010). Highly Hydrophilic and Low-Protein-Fouling Polypropylene Membrane Prepared by Surface Modification with Sulfobetaine-Based Zwitterionic Polymer through a Combined Surface Polymerization Method. *J. Membr. Sci.* 362 (1), 326–333. doi:10.1016/j.memsci.2010.06.037

Zheng, C., and Huang, Z. (2019). Self-assembly of Hydrophobic Associating Polyacrylamide Prepared by Aqueous Dispersion Polymerization. *J. Dispersion Sci. Tech.* 40 (9), 1317–1325. doi:10.1080/01932691.2018.1511434

Zhu, Z., Kang, W., Yang, H., Wang, P., Zhang, X., Yin, X., et al. (2017). Study on Salt Thickening Mechanism of the Amphiphilic Polymer with Betaine Zwitterionic Group by β-cyclodextrin Inclusion Method. *Colloid Polym. Sci.* 295 (10), 1887–1895. doi:10.1007/s00396-017-4169-7